Nonlinear behavior of the band gap of $Pb_{1-x}Eu_xSe$ $(0 \leq x \leq 1)$ from first principles

Andreas Grüneis, Kerstin Hummer, Martijn Marsman,* and Georg Kresse
Faculty of Physics, Universität Wien and Center for Computational Materials Science, Sensengasse 8/12, A-1090 Vienna, Austria
(Received 28 March 2008; revised manuscript received 29 July 2008; published 3 October 2008)

We present an *ab initio* investigation of the band gap of the $Pb_{1-x}Eu_xSe$ $(0 \leq x \leq 1)$ alloy using the special quasirandom structure approach proposed by Wei *et al.* [Phys. Rev. B **42**, 9622 (1990)]. Due to the complexity of this particular system, i.e., (i) the narrow-band gap of the parent compound PbSe, (ii) spin-orbit coupling induced by relativistic effects in the Pb atoms, and (iii) the strongly localized f electrons of Eu, an accurate description of its properties represents a serious challenge to density-functional theory. We discuss results obtained from Perdew, Burke, and Ernzerhof density functional and Heyd, Scuseria, and Ernzerhof Hartree-Fock hybrid functional calculations, both with and without an additional Hubbard U treatment of the Eu f electrons. At low Eu concentrations $(x < 0.13)$ the HSE functional gives a good description of the band gap of $Pb_{1-x}Eu_xSe$. At high Eu concentrations an additional Hubbard U treatment of the Eu f electrons is mandatory.

DOI: 10.1103/PhysRevB.78.165103 PACS number(s): 71.15.Mb, 71.20.Nr

I. INTRODUCTION

PbSe belongs to the lead chalcogenides (Pb X: X=S, Se, Te), which are narrow-gap IV-VI semiconductors. Pb X attracts a lot of interest due to their unique physical properties: (i) direct fundamental band gaps of only a few hundred meVs ($E_g < 500$ meV), (ii) extremely high static dielectric constants, (iii) a large positive temperature coefficient $(\partial E_g/\partial T > 0)$ of the band gaps due to strong electron-phonon interactions, and (iv) a negative pressure dependence $(\partial E_g/\partial p < 0)$.[1] These properties make them and their alloys with europium (Eu) or tin (Sn) suitable materials for midinfrared emitters and detectors.[2–4] For example, they find technological application in long-wavelength imaging devices[5] and thermophotovoltaic energy converters.[6] Furthermore, an outstanding achievement in this field of optoelectronic developments is the realization of the first midinfrared quantum-dot laser with PbSe and PbEuTe layers in the active region.[7] This has motivated various elaborate theoretical investigations of the PbX on different levels of approximations[8–11] as well as experimental studies,[12–15] which revealed new and interesting insights into the physics of these materials. For recent theoretical work, the reader is referred to Ref. 16, whereas recent experimental results are summarized in Ref. 17.

EuSe is a magnetic semiconductor, on account of its half-filled $4f$ band. Different magnetic phases have been reported for EuSe,[18] ranging from antiferromagnetic ordering (below T_N=1.8 K) and low magnetic field to mixed phases with antiferromagnetic and ferrimagnetic orderings (below 2.8 K) and ferromagnetic ordering at high magnetic field. At 4 K and high magnetic fields EuSe has proven its applicability as spin aligner in an Ag/EuSe/Al junction,[19] with which a spin polarization of the tunneling electrons higher than 90% can be achieved. Its practical applicability in spintronics,[20] however, is limited since the magnetic ordering occurs only at very low temperatures.

Both PbSe and EuSe crystallize in the rock salt structure. PbSe exhibits a direct fundamental band gap of 278 meV at room temperature[21] at the L point (Brillouin-zone boundary). EuSe is characterized by an indirect band gap of 1.8–1.9 eV,[21,22] with the valence-band maximum (VBM) located at Γ and the conduction-band minimum (CBM) at X. The valence-band edge is made up of Eu-$4f$ states.[22]

It is common practice in the materials engineering of optoelectronic devices to dope narrow-gap semiconductors with magnetic ions or to alloy them with magnetic semiconductors.[3] The significant difference in the magnitude of the band gaps in PbSe and EuSe combined with their similar structural properties (lattice constants and space group) allows to tune the band gap by alloying these materials. In the case of the $Pb_{1-x}Eu_xSe$ system, an increasing Eu concentration x leads to an opening of the gap. To the best of our knowledge, only the low Eu concentration range $(x \leq 0.1)$ has been experimentally investigated so far, revealing a steep initial slope $\partial E_g/\partial x = 3900$ meV/mole.[23] $\partial E_g/\partial x$ at small x is too large to be consistent with an assumed simple linear dependence of the band gap over the entire range $0 \leq x \leq 1$. This shows that the band gap of $Pb_{1-x}Eu_xSe$ as a function of x must exhibit a strong nonlinear behavior. The calculations presented in this work explicitly demonstrate this nonlinear behavior of the $Pb_{1-x}Eu_xSe$ band gap at higher Eu doping concentrations.

Our approach relies on density-functional theory (DFT) using several different approximations to the exchange-correlation (XC) interaction. Standard (semi)local XC functionals such as the Perdew, Burke, and Ernzerhof (PBE) parametrization of the generalized gradient approximation (GGA) fail to yield the correct band gap in both parent materials. In the case of PbSe, PBE band-structure calculations show the band character to be inverted at the L point, when relativistic effects are properly treated by including spin-orbit coupling (SOC).[16] In EuSe, the spin splitting within the $4f$ shell is severely underestimated in PBE calculations. As a result, the $4f$ states cross the Fermi level yielding a metallic ground state.

To overcome these problems it is necessary to go beyond standard DFT. In the case of EuSe, a Hubbard U term may be introduced in order to increase the spin splitting within the $4f$ shell,[24] i.e., pull the occupied $4f$ states below the Fermi level and open up the band gap of EuSe. This DFT $+U$ approach, however, still underestimates the EuSe band gap $[E_g(\text{PBE}+U)=1.3$ eV for $U=6.7$ eV, compared to

$E_g(\text{exp})=1.9$ eV]. Increasing U, the strength of the effective Coulomb interaction within the $4f$ manifold, does not open up the gap any further, since the $4f$ states simply drop below the high lying Se p states,[22] which then make up the top of the valence band. Ghosh *et al.*[24] achieve a further increase in the EuSe band gap by introducing additional Hubbard U terms to shift these Se-p states down and to push the conduction bands, which mainly consist of Eu-d states, up. Although DFT+U is well justified for localized electrons such as f states, the approach is principally problematic for bandlike states, e.g., the Se-p states.

Recently, it has been shown that the screened Hartree-Fock (HF) density-functional hybrid proposed by Heyd, Scuseria, and Ernzerhof[25–30] (HSE) presents a significant improvement over (semi)local-density functionals, such as PBE, for the prediction of accurate band gaps in many solids.[28,31,32] We show here that the HSE functional does indeed provide a better description of the EuSe band gap than the PBE functional: the $4f$ states are more strongly bound. However, to obtain satisfactory agreement with experiment, the inclusion of a Hubbard U term acting on the Eu $4f$ electrons is still required. Additionally, we present single-shot GW (Refs. 33–35) (G_0W_0) calculations (using HSE wave functions) of the quasiparticle band structure of the two parent compounds.

In short, the main motivation for this work is to arrive at an accurate first-principles description of the band gaps of the alloy $Pb_{1-x}Eu_xSe$ as well as its parent compounds PbSe and EuSe. Moreover, a qualitative explanation for its nonlinear dependence on the Eu concentration will be given.

II. THEORETICAL APPROACH

A. Computational details

All theoretical results presented in this work were obtained with the Vienna *ab initio* simulation package[36] (VASP) within the framework of the projector-augmented-wave (PAW) method[37] using a plane-wave basis set. The band structure of PbSe was calculated using the PBE (Ref. 38) semilocal-density functional and the HSE (Ref. 25) screened HF/DFT hybrid functional. We use a variant of the HSE06 functional that observes the homogeneous electron-gas limit and all important sum rules. Contrary to the conventional HSE06 functional,[25–27] the screening parameter is set to $\omega=0.300$ Å^{-1} in both the semilocal as well as nonlocal part of the exchange functional, whereas the recommended choice is $\omega=0.207$ Å^{-1}. As has been shown previously, the specific choice of the screening parameter ω has very little influence on the total energies, but slightly affects band gaps.[27,32,39] From now on we will refer to this particular functional as HSE.

The Pb ($5d^{10}6s^26p^2$), Eu ($4f^75s^25p^66s^2$), and Se ($4s^24p^4$) states were treated as valence states, while the remaining states were kept frozen. A plane-wave cutoff energy of 300 eV was used in all calculations. At this energy cutoff the EuSe band gaps are converged with respect to size of the plane-wave basis set to within 30 meV.

For the calculations on EuSe an additional Hubbard U term, acting on the Eu $4f$ manifold, was added to the aforementioned functionals, in accordance with the rotationally invariant form of DFT+U proposed by Liechtenstein *et al.*[40] The PBE+U calculations were done with $U=6.7$ eV and $J=0.7$ eV, i.e., identical to the parameters that were optimized for Gd^{3+} (which is isolectronic to Eu^{2+}).[41] In the HSE+U calculations we used $U=4.9$ eV and $J=0.7$ eV (these parameters provide optimal agreement between the theoretical and experimental EuSe band gaps). The G_0W_0 calculations of the PbSe and EuSe quasiparticle band structures were done using HSE wave functions, since recent work shows this to be superior to single-shot GW using PBE wave functions.[42] Also this approach surmounts any problems occurring for materials which DFT predicts to be metallic, whereas they are semiconductors experimentally.[42] In the case of EuSe, we considered the ferromagnetic ground state only.

The Brillouin-zone integrations have been carried out on $(8\times8\times8)$ Γ-centered k meshes for the face-centered cubic primitive cells of EuSe and PbSe. Convergence tests at the PBE($+U$) level, using $(12\times12\times12)$ Γ-centered k meshes, show the PbSe (EuSe) band gaps to be converged to within a few meV. For the special quasirandom structures (SQS) used in the calculations of $Pb_{1-x}Eu_xSe$ $(0<x<1)$ $(4\times4\times1)$, $(3\times3\times1)$, and $(2\times2\times1)$ Γ-centered k meshes were used for SQS8, SQS12, and SQS14, respectively. These k meshes are sufficiently dense to reproduce the band gaps of the parent compounds (i.e., $x=0$ and $x=1$) using the respective quasirandom supercells to within 2 meV.

Since the low-temperature lattice constant and band gap of EuSe are not known from experiment, the band-structure calculations on the parent compounds were performed at the experimental equilibrium lattice constants at ambient conditions. These are $a=6.124$ Å and $a=6.190$ Å for PbSe and EuSe, respectively.[21] Results for PbSe at the low-temperature lattice constant have also been published before using a similar setup as employed in the present work.[16]

The experimental investigation of E_g as a function of the Eu concentration, on the other hand, was carried out at low temperature. The theoretical calculations for the compounds were performed (i) at the low-temperature lattice constant of PbSe $a=6.098$ Å (ii) and at a series of lattice constants linearly interpolated between the PbSe lattice constant $a=6.098$ Å and the EuSe lattice constant $a=6.190$ Å (the low-temperature lattice constant of EuSe is not known experimentally). This allows to disentangle alloying and lattice expansion effects.

The HSE+SOC and PBE+SOC lattice constants of PbSe are $a=6.170$ Å and $a=6.214$ Å, respectively.[16] The mismatch between the theoretical and experimental (low temperature) PbSe lattice constants amounts to 1.2% (HSE+SOC) and 1.9% (PBE+SOC). In this case, HSE yields better agreement with experiment.

The PBE+U, HSE, and HSE+U lattice constants of EuSe are $a=6.201$ Å, $a=6.226$ Å, and $a=6.243$ Å, respectively; between 0.2% (PBE+U) and 0.8% (HSE+U) larger than the experimental lattice constant of EuSe, but all in very reasonable agreement with experiment. We note that EuSe has a much too small lattice constant using PBE because f electrons are located at the Fermi-level yielding an unphysical binding contribution. PBE+U only partly corrects for this,

TABLE I. The lattice vectors of SQS in units of $a/2$, where a is the lattice constant of PbSe (a=6.098 Å).

Structure	Lattice vectors		
SQS8	(−1,−2,1)	(5,5,2)	(−2,−1,1)
SQS12	(2,1,3)	(1,2,3)	(−4,−4,0)
SQS14	(2,−1,−1)	(2,0,2)	(−1,4,1)

whereas HSE yields a similar and consistent overestimation of the lattice constant as for PbSe.

B. Special quasirandom structures

Following Wei *et al.*,[43] the alloy is modeled by means of special quasirandom structures: supercells that are chosen in such a way as to best mimic a perfect $Pb_{1-x}Eu_xSe$ random alloy. The degree to which the first few radial correlation functions of the SQS match those of an infinite perfect random alloy is taken as a measure of its quality.

Table I lists the lattice vectors of the SQS used in the present work. These structures are equivalent to the corresponding SQS8, SQS12, and SQS14 supercells (for x=0.5) in Ref. 43. For Eu concentrations other than x=0.5 the lattice vectors were kept fixed, and the lattice site occupancies (by either Eu or Pb atoms) were optimized to best match the radial pair-correlation functions of the random alloy.

For a perfect binary random alloy the radial pair-correlation function for the mth nearest neighbor, is given by[43]

$$\bar{\Pi}_{2,m}^{\text{perfect}} = (2x-1)^2. \tag{1}$$

For concentrations other than x=0.5, we generated all possible configurations of the SQS8, SQS12, and SQS14 supercells (consistent with a particular concentration) and calculated the radial pair-correlation functions $\bar{\Pi}_{2,m}$, for m=1, 2, 3, and 4. The structures that showed the smallest deviation from the perfect random alloy were used for further calculations. As a measure for the deviation we took the following expression:

$$\sqrt{\sum_{m=1}^{4} (\bar{\Pi}_{2,m}^{\text{perfect}} - \bar{\Pi}_{2,m})^2}, \tag{2}$$

which will be referred to as "error" in the following. Table II lists the radial pair-correlation functions and the corresponding errors for the SQS used in the present work.

III. RESULTS AND DISCUSSION

A. Electronic properties of PbSe and EuSe

Recent *ab initio* calculations on the lead chalcogenides show the HSE hybrid functional to clearly outperform the standard PBE functional for the description of the electronic properties of these narrow-gap semiconductors.[16] In particular, band structure, band gaps, and effective charge-carrier masses are in good agreement with experiment. For the sake of clarity of the following discussion on the band gap of $Pb_{1-x}Eu_xSe$, the band-structure calculations of PbSe are included here as well and the main conclusions from Ref. 16 are briefly recapitulated.

In Fig. 1 the band structure of PbSe obtained from HSE and PBE calculations that include SOC is depicted. The band dispersions are shown along the high-symmetry lines from Γ to L to W in the first Brillouin zone. From the size of the symbols in Fig. 1, the character of the electronic states at different k vectors and energies can be seen. As is clearly shown in Fig. 1 the direct fundamental band gap is located at the L point. In the PBE+SOC case, however, the band character is inverted in the vicinity of L (see left panel of Fig. 1) resulting in a "negative" band gap. The HSE+SOC calculations yield the correct band order. The valence states mainly consist of anion (Se) p states that hybridize with cation (Pb) s states, whereas the conduction bands have mainly Pb-p and Se-s characters. Furthermore, HSE+SOC yields a quantitatively improved prediction of the PbSe band gap compared to the PBE ($E_g^{\text{HSE+SOC}}$=139 meV vs $E_g^{\text{PBE+SOC}}$=−115 meV). The underestimation of the band gap compared to experiment (E_g^{exp}=275 meV) may be attributed to strong electron-phonon coupling that gives rise to the peculiar positive and very pronounced temperature dependence of the gap. Note in this context that the band gap at low temperature is well

TABLE II. Radial pair-correlation functions $\bar{\Pi}_{2,m}$ for m=1, 2, 3, and 4, and the error with respect to the perfect random alloy, for different concentrations x.

Structure	x	$\bar{\Pi}_{2,1}$	$\bar{\Pi}_{2,2}$	$\bar{\Pi}_{2,3}$	$\bar{\Pi}_{2,4}$	$\bar{\Pi}_{2,m}^{\text{perfect}}$	Error
SQS14	0.071	0.714	0.714	0.738	0.762	0.735	0.0398
SQS12	0.083	0.742	0.690	0.690	0.742	0.694	0.0676
SQS8	0.125	0.583	0.500	0.583	0.583	0.563	0.0722
SQS8	0.25	0.167	0.167	0.333	0.167	0.25	0.1667
SQS8	0.375	0.0	0.0	0.083	0.083	0.063	0.0932
SQS8	0.5	0.0	0.0	0.04	−0.08	0.0	0.0932
SQS8	0.625	0.0	0.0	0.083	0.083	0.063	0.0932
SQS8	0.75	0.167	0.167	0.333	0.167	0.25	0.1667
SQS8	0.875	0.583	0.500	0.583	0.583	0.563	0.0722

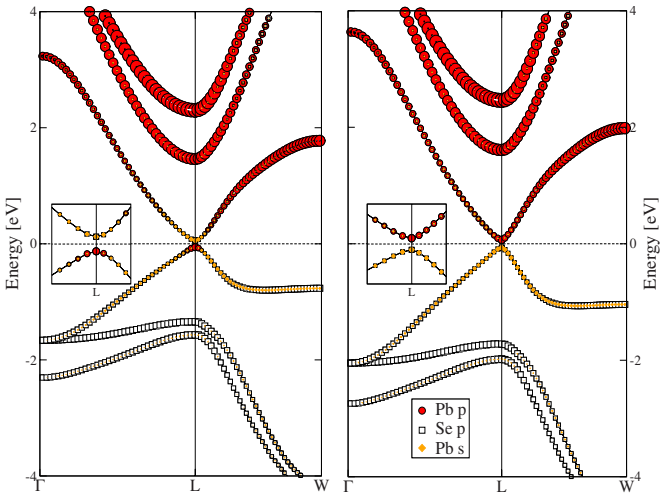

FIG. 1. (Color online) Band structure of PbSe obtained from PBE (left) and HSE (right) calculations taking spin-orbit-coupling into account. The size of the symbols reflects the character of the electronic states. The insets show an enlargement of the valence and conduction bands in the vicinity of the L point.

reproduced by HSE+SOC calculations as was shown in Ref. 16.

In contrast to PbSe, EuSe exhibits an indirect band gap. As can be seen from the PBE+U, HSE, and the HSE+U band structures depicted in Figs. 2 and 3, the VBM is located at Γ and the CBM at X. The VBM mainly consists of Eu-f states and the CBM of Eu-d states. Furthermore, the Se-p bands also belong to the valence-band region and are close to the Eu-f manifold. These findings are consistent with other calculations and experimental findings reported in Refs. 22, 24, and 44.

The EuSe PBE+U band gap ($E_g^{\mathrm{PBE}+U}=1.3$ eV) is still 30% too small compared to experiment ($E_g^{\mathrm{exp}}=1.9$ eV). A further increase of the Hubbard U will not improve the result, since then the Eu-f electrons drop below the Se-p states. Thus, the valence-band maximum would be formed by Se-p states without increasing the band gap further. This can be recognized in the upper panel of Fig. 2 from the fact that the energy difference between the Se-p states at Γ and the Eu-d states at X, $E_{g,p-d}^{\mathrm{PBE}+U}=1.4$ eV is only slightly larger than the gap $E_g^{\mathrm{PBE}+U}=1.3$ eV between the Eu-f and d states.

As shown in the lower panel of Fig. 2, the grave underestimation of the HSE EuSe band gap ($E_g^{\mathrm{HSE}}=0.7$ eV) with respect to experiment, is primarily due the fact that the Eu-f states lie too close to the Fermi level. Compared to the PBE+U results, the HSE functional, however, does provide an improved description of the energy difference between the Se-p and Eu-d states $E_{g,p-d}^{\mathrm{HSE}}=2.3$ eV (from experiment $E_{g,p-d}^{\mathrm{exp}}=3.1\pm0.3$ eV).[22] Due to the reasonable description of the $p-d$ gap, a HSE+U ($U=4.9$ eV and $J=0.7$ eV) calculation of the band gap in EuSe can reach almost perfect agreement with experiment $E_g^{\mathrm{HSE}+U}=1.9$ eV (see Fig. 3). In both the PBE+U as well as the HSE+U calculations hybridization between the Se-p and the Eu-f states in the valence band is observed and the dispersion of the Eu-f bands is resultantly stronger than in the HSE case.

Unfortunately G_0W_0 (single-shot GW) calculations starting from HSE wave functions have even more pronounced

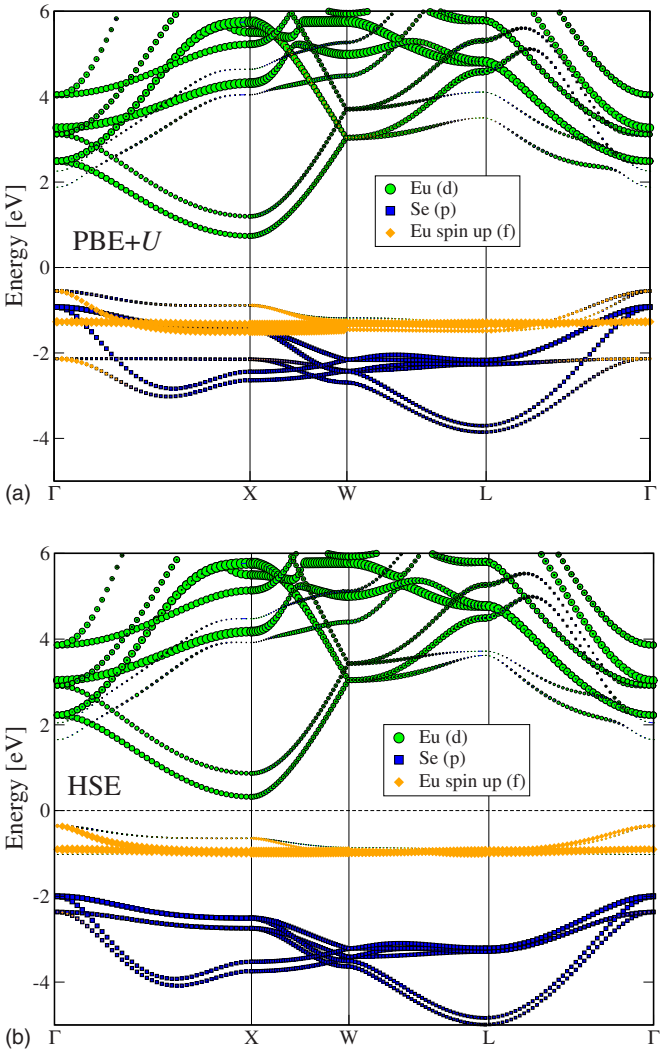

FIG. 2. (Color online) Band structure of EuSe obtained from PBE+U and HSE calculations. The size of the symbols reflects the character of the electronic states.

troubles describing the strongly localized Eu-f states than HSE. Resultantly, the EuSe band gap is seriously underestimated within the G_0W_0 approximation $E_g^{G_0W_0}=0.4$ eV. The G_0W_0 energy difference between the Se-p and Eu-d states $E_{g,p-d}^{G_0W_0}=2.9$ eV, however, does present an improvement over the HSE description and is in excellent agreement with experiment. Problems for the description of localized states (Eu 4f in the present case) are well documented, in particular for 3d compounds such as ZnO, ZnS, or GaAs. See for instance Refs. 35 and 45–47.

The aforementioned PbSe and EuSe energy gaps are summarized and compared to experimental findings in Table III.

B. Nonlinear behavior of the band gap of $Pb_{1-x}Eu_xSe$

In Sec. III A, it was demonstrated that the HSE functional gives a reasonable account of the electronic properties, in particular if the Eu 4f shell is treated using a Mott Hubbard U. Here we present results regarding the dependence of the energy gap of the random alloy $Pb_{1-x}Eu_xSe$, on the Eu con-

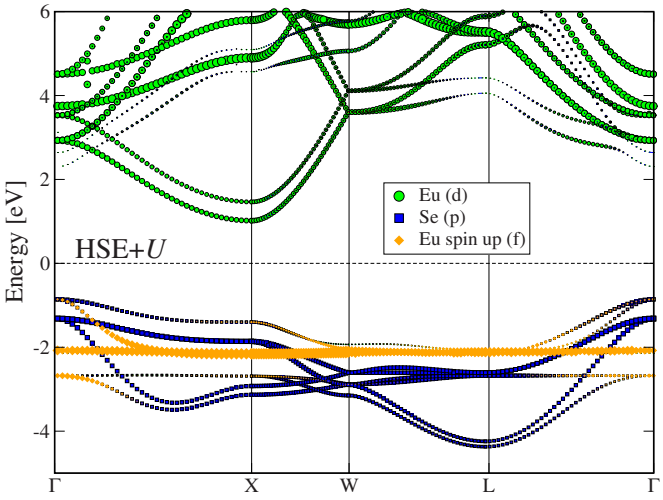

FIG. 3. (Color online) Band structure of EuSe obtained from HSE+U calculations. The size of the symbols reflects the character of the electronic states.

centration x. The first part of this section focuses on the low Eu concentration range $x<0.13$, where experimental data are available for comparison. In the second part, results for larger x are presented.

1. Concentration regime $x<0.13$

Figure 4 shows PBE+U and HSE+SOC(+U) $Pb_{1-x}Eu_xSe$ band gaps together with experimental results.[23] Be aware that the PBE+U values correspond to calculations without SOC, in order to avoid the band inversion at the L point and a concomitantly interchanged band character for PbSe ($x=0$). The results for Eu concentrations $x=7.14\%$, 8.33%, and 12.5% were obtained using SQS14, SQS12, and SQS8 special quasirandom structures, respectively. Also shown in Fig. 4 are linear least square fits to the PBE+U (dash-dotted line), HSE+SOC (dashed line), and experimental results (full line). The linear least square fit to the HSE+SOC data is given by $E_g(x)=3900x+120$ (E_g in meV, x in mole^{-1}), with a slope of $\partial E_g/\partial x=3900$ meV/mole, in excellent agreement with the fit to the experimental data $E_g(x)=3900x+150$. At these low concentrations the band gap shows hardly any dependence on the Hubbard U as shown by the single HSE+SOC+U data point for $x=12.5\%$ in Fig. 4.

TABLE III. Energy gap E_g of PbSe and EuSe as obtained from different methods at ambient experimental volumes. $E_{g,p-d}$ is the energy gap between Se-p and Eu-d states.

	PbSe	
	E_g **[eV]**	
PBE+SOC	−0.11	
HSE	0.58	
HSE+SOC	0.14	
G_0W_0 (HSE)	0.63	
G_0W_0(HSE)+ΔSOC	0.19	
Expt.	0.28	
	EuSe	
	E_g [eV]	$E_{g,p-d}$ [eV]
PBE+U	1.3	1.4
HSE	0.7	2.3
HSE+U	1.9	2.3
G_0W_0 (HSE)	0.4	2.9
Expt.	1.9	3.1 ± 0.3

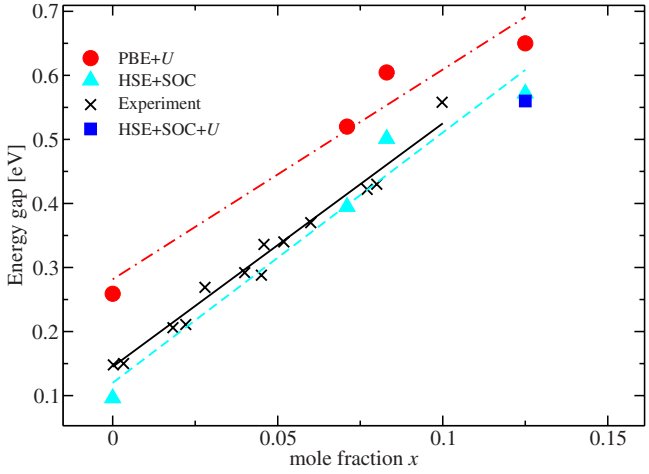

FIG. 4. (Color online) $Pb_{1-x}Eu_xSe$ band gaps from PBE+U and HSE+SOC(+U) calculations and from experiment for low Eu concentrations ($x<0.13$). The calculations were performed at the experimental low-temperature lattice constant of PbSe $a=6.098$ Å. The lines represent linear least square fits to the respective data. Experimental data were taken from Ref. 23.

The linear fit to the PBE+U data $E_g(x)=3400x+280$ presents a slight underestimation of $\partial E_g/\partial x$. This discrepancy may be attributed to the neglect of SOC in these calculations as will be demonstrated in Sec. III B 2.

In all calculations within the low-concentration regime the gap remained direct and at the L point.

2. Concentration regime $0.13<x\leq 1$

Figure 5 shows the PBE+U, HSE+SOC, and HSE+SOC+U band gaps of $Pb_{1-x}Eu_xSe$ as a function of the Eu concentration x for $x>12.5\%$. The calculations were performed at the experimental low-temperature lattice constant of PbSe ($a=6.098$ Å) and using an interpolation between the PbSe and EuSe lattice constants ($a=6.190$ Å) according to Vegard's law. Note that the results for small Eu concentrations are hardly changed by using Vegard's law, confirming that the lattice expansion effect is negligible in the low-concentration regime considered in Sec. III B 1.

The overall behavior of the gap is similar in all three approaches. For $x<0.5$ the band gap increases with increasing Eu concentration, between $0.5<x<0.8$ the band gap saturates, and for $x>0.8$ it decreases. The gap reaches a maximum around a concentration of 75%, if lattice expansion is taken into account.

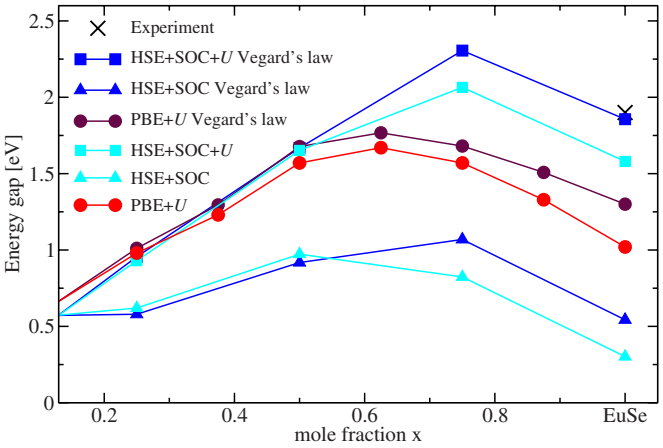

FIG. 5. (Color online) $Pb_{1-x}Eu_xSe$ band gaps using PBE+U and HSE+SOC(+U) calculations for low Eu concentrations $0.125 < x \leq 1$. The experimental EuSe band gap was taken from Ref. 22. The calculations were performed at the experimental low-temperature lattice constant of PbSe (a=6.098 Å) and using a linear interpolation between the PbSe and EuSe volumes (a=6.190 Å) according to Vegard's law.

As we have already emphasized, the band gap is hardly influenced by the volume up to Eu concentrations around 50%. In this doping regime, the band gap remains at the L point, and this suggests that the band gap at the L point is not very sensitive to the volume. At higher Eu concentration the band gap is indirect between Γ and X, similar as in EuSe (see below). Clearly, the indirect gap is far more sensitive to the volume and changes by almost 0.3 eV upon a lattice-constant change of 1.5%.

To elucidate the origin of the aforementioned nonlinear behavior of the $Pb_{1-x}Eu_xSe$ band gap, the valence-band energies at Γ and L [$\epsilon_V(\Gamma)$ and $\epsilon_V(L)$] and the conduction-band energies at X and L [$\epsilon_C(X)$ and $\epsilon_C(L)$] as a function of x were approximated by linearly interpolating them between PbSe (x=0) and EuSe (x=1). The result is shown in Fig. 6. The eigenenergies plotted in Fig. 6 were taken from HSE+U calculations at the low-temperature PbSe lattice constant a =6.098 Å for both PbSe as well as EuSe. The band energies of the two materials were aligned at $\epsilon_V(L)$, but a different choice would not change the band-gap variation (gray shaded area). Despite its simplicity, the approximation allows for a qualitative explanation of the nonlinear behavior of the $Pb_{1-x}Eu_xSe$ band gap. For Eu concentrations smaller than 50% a steep increase of E_g is expected. Between 0.5 $< x < 0.7$ the band gap saturates and finally decreases for $x > 0.7$.

Moreover, the VBM is shown to change from L to Γ around x=0.7 in accord with the full *ab initio* calculations. Figure 6 also predicts the CBM to switch from L to X at x =0.5. Hence, our simple approximation predicts a change from a direct ($L \rightarrow L$) to an indirect gap ($L \rightarrow X$) at an Eu concentration of 50% and an additional change to an indirect ($\Gamma \rightarrow X$) gap at x=0.7. Unfortunately, in the first BZ of the PbSe and EuSe parent compounds, the L and X points are no longer distinguishable in the reciprocal space of the SQS8 structure (both are folded onto Γ), i.e., from our calculations we cannot easily determine the Eu concentration at which the

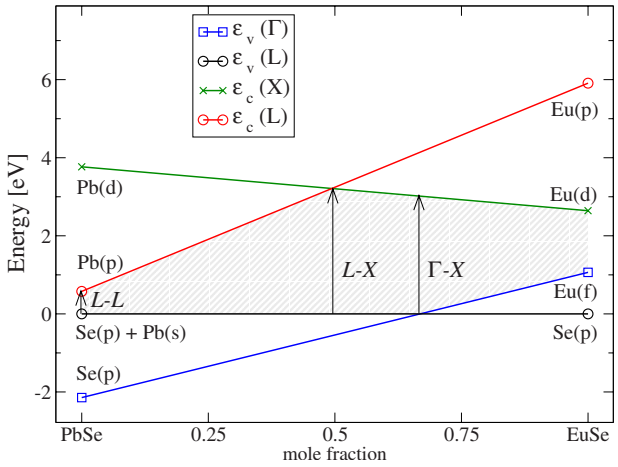

FIG. 6. (Color online) A linear interpolation between the PbSe (x=0) and EuSe (x=1) valence-band energies at Γ and L [$\epsilon_V(\Gamma)$ and $\epsilon_V(L)$] and the conduction-band energies at X and L [$\epsilon_C(X)$ and $\epsilon_C(L)$]. The gray shaded area should approximate the band gap of the alloy.

CBM switches from L to X. In addition, Fig. 6 shows the band character of the corresponding states at x=0 and x=1 [Pb(s), Pb(p), Pb(d), Se(p), Eu(p), Eu(d), and Eu(f)].

In Fig. 7 we illustrate the effect of relaxing the atomic positions in the SQS approach. In Ref. 43 the atomic positions have been optimized for all applied SQS (Ga_2AsP). However, due to the large computational effort required for such relaxations on the HSE+SOC level, the optimization of the atomic position has been omitted in the present work. To test how this approximation affects the results, the energy gap of $Pb_{1-x}Eu_xSe$ with relaxed atomic positions has been computed using PBE+U for $0.125 \leq x \leq 0.875$. The results of these calculations are compared to the previous findings for the unrelaxed structures in Fig. 7. On the PBE+U level, only small changes in the energy gap are found (0.2 eV). We hence conclude that the effects of relaxation are small and can be safely neglected for the present qualitative discussion.

Finally, HSE band gaps without SOC are shown in Fig. 7, and, as reference, again the HSE band gaps including SOC.

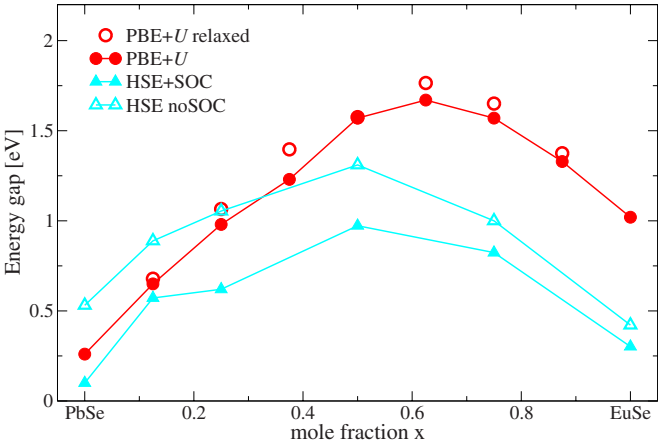

FIG. 7. (Color online) $Pb_{1-x}Eu_xSe$ band gaps obtained from PBE+U calculations with and without relaxed atomic positions and the HSE energy gaps with and without taking SOC into account are plotted.

As one might expect, the effect of SOC, i.e., reducing the energy gap, becomes less pronounced with increasing Eu concentration. Moreover, Fig. 7 shows that SOC slightly increases the initial slope. In particular, the energy gaps obtained using HSE show a steeper increase with respect to x if SOC is included.

IV. CONCLUSION

In this work, we have presented *ab initio* results for the energy gap of the $Pb_{1-x}Eu_xSe$ alloy as a function of the Eu concentration, as well as the band structures of PbSe and EuSe. The alloy was modeled by means of special quasirandom structures. We show that the PBE functional fails in the description of both parent compounds, with an inverted band gap for PbSe and a predicted metallic behavior for EuSe. PBE+U improves the results for EuSe by lowering the occupied Eu-f states and shifting the unoccupied Eu-f states above the conduction-band onset, but of course, the description of PbSe is not improved.

Overall, the hybrid functional HSE provides a better starting point for the description of the electronic properties of both parent compounds. The predicted band gap of PbSe is in very good agreement with experiment, and for EuSe the energy difference between the Se-p states and Eu-d states is in reasonable agreement with experiment. However, although HSE predicts an insulating behavior for EuSe (in accord with experiment) the splitting between the occupied and unoccupied f states is underestimated. Using one quarter of the exact exchange, the exchange splitting within the f manifold is obviously too small. Hence, there is still a need to include a Hubbard U to further increase the energy difference between the occupied and unoccupied f manifolds. Upon empirically introducing a U of 4.9 eV, good agreement with experiment is obtained for EuSe. Although this *ad hoc* procedure is certainly somewhat unsatisfactory, no *ab initio* method (not even *GW*, see Sec. III A) is presently capable to accurately predict the exact position of the f states.

Application of the HSE+U method to the $Pb_{1-x}Eu_xSe$ alloy should allow for an accurate evaluation of the band-gap variation. Indeed, the initial slope of the band gap with respect to the Eu content is in excellent agreement with experiment ($\partial E_g/\partial x = 3900$ meV/mole). With increasing Eu content we observe a change from a direct band gap at the L point to an indirect band gap between Γ and L. At the same time the band gap reaches a maximum and further on decreases with increasing Eu content. This peculiar behavior can be understood resorting to a rather simple model, where one assumes that at all high-symmetry points the quasiparticle energies are simple linear interpolations between the quasiparticle energies of the parent compounds. This model explains both the change from a direct to an indirect band gap and the maximum band gap around an Eu content of 0.5–0.7 mole.

Since the above results are very promising, future prospects will include *ab initio* studies of interface structures consisting of layers of alloys and pure bulk materials, e.g., $PbSe/Pb_{1-x}Eu_xSe$, which is particular important for the mid-infrared quantum dot laser technology.

ACKNOWLEDGMENTS

This work has been supported by the Austrian Fonds zur Förderung der wissenschaftlichen Forschung within the special research program Infrared Optical Nanostructures (IR-ON) and the START Project No. Y-218.

*martijn.marsman@univie.ac.at

[1] R. Dornhaus, G. Nimtz, and B. Schlicht, *Narrow-Gap Semiconductors* (Springer-Verlag, Berlin, 1985).
[2] H. Krenn, S. Yuan, N. Frank, and G. Bauer, Phys. Rev. B **57**, 2393 (1998).
[3] T. C. McGill and D. A. Collins, Semicond. Sci. Technol. **8**, S1 (1993).
[4] H. Pascher and G. Bauer, *Lead Chalcogenides: Physics and Applications* (Taylor & Francis, New York, 2003), Vol. 18.
[5] H. Zogg, A. Fach, J. John, J. Masek, P. Muller, C. Paglino, and W. Buttler, Opt. Eng. **33**, 1440 (1994).
[6] T. K. Chaudhuri, Int. J. Energy Res. **16**, 481 (1992).
[7] G. Springholz, T. Schwarzl, W. Heiss, G. Bauer, M. Aigle, H. Pascher, and I. Vavra, Appl. Phys. Lett. **79**, 1225 (2001).
[8] D. L. Mitchell and R. F. Wallis, Phys. Rev. **151**, 581 (1966).
[9] M. Schlüter, G. Martinez, and M. L. Cohen, Phys. Rev. B **12**, 650 (1975).
[10] S.-H. Wei and A. Zunger, Phys. Rev. B **55**, 13605 (1997).
[11] E. A. Albanesi, C. M. I. Okoye, C. O. Rodriguez, E. L. Peltzer y Blanca, and A. G. Petukhov, Phys. Rev. B **61**, 16589 (2000).
[12] J. N. Zemel, D. Jensen, and R. B. Schoolar, Phys. Rev. **140**, A330 (1965).
[13] S. E. Kohn, P. Y. Yu, Y. Petroff, Y. R. Shen, Y. Tsang, and M. L. Cohen, Phys. Rev. B **8**, 1477 (1973).
[14] T. Grandke, L. Ley, and M. Cardona, Phys. Rev. B **18**, 3847 (1978).
[15] V. Hinkel, H. Haak, C. Mariani, L. Sorba, K. Horn, and N. E. Christensen, Phys. Rev. B **40**, 5549 (1989).
[16] K. Hummer, A. Grüneis, and G. Kresse, Phys. Rev. B **75**, 195211 (2007).
[17] I. I. Zasavitskii, E. A. de Andrada e Silva, E. Abramof, and P. J. McCann, Phys. Rev. B **70**, 115302 (2004).
[18] R. Griessen, M. Landolt, and H. R. Ott, Solid State Commun. **9**, 2219 (1971).
[19] J. S. Moodera, R. Meservey, and X. Hao, Phys. Rev. Lett. **70**, 853 (1993).
[20] S. A. Wolf, D. D. Awschalom, R. A. Buhrman, J. M. Daughton, S. von Molnár, M. L. Roukes, A. Y. Chtchelkanova, and D. M. Treger, Science **294**, 1488 (2001).
[21] *Semiconductors*: Group IV Elements, IV-IV and III-IV Compounds, Landolt-Börnstein, New Series, Group III, Vol. 41, Pt. A, edited by O. Madelung, U. Rössler, and M. Schulz (Springer-Verlag, Berlin, 2005).
[22] D. E. Eastman, F. Holtzberg, and S. Methfessel, Phys. Rev. Lett. **23**, 226 (1969).
[23] J. W. Tomm, K.-P. Möllmann, F. Peuker, K. H. Herrmann, H.

Böttner, and M. Tacke, Semicond. Sci. Technol. **9**, 1033 (1994).
[24] D. B. Ghosh, M. De, and S. K. De, Phys. Rev. B **70**, 115211 (2004).
[25] J. Heyd, G. E. Scuseria, and M. Ernzerhof, J. Chem. Phys. **118**, 8207 (2003).
[26] J. Heyd, G. E. Scuseria, and M. Ernzerhof, J. Chem. Phys. **124**, 219906 (2006).
[27] A. V. Krukau, O. A. Vydrov, A. F. Izmaylov, and G. E. Scuseria, J. Chem. Phys. **125**, 224106 (2006).
[28] J. Heyd and G. E. Scuseria, J. Chem. Phys. **121**, 1187 (2004).
[29] J. Heyd, J. E. Peralta, G. E. Scuseria, and R. L. Martin, J. Chem. Phys. **123**, 174101 (2005).
[30] J. E. Peralta, J. Heyd, G. E. Scuseria, and R. L. Martin, Phys. Rev. B **74**, 073101 (2006).
[31] J. Paier, M. Marsman, K. Hummer, I. C. Gerber, J. G. Angyan, and G. Kresse, J. Chem. Phys. **124**, 154709 (2006).
[32] J. Paier, M. Marsman, K. Hummer, G. Kresse, I. C. Gerber, and J. G. Ángyán, J. Chem. Phys. **125**, 249901 (2006).
[33] L. Hedin, Phys. Rev. **139**, A796 (1965).
[34] G. Onida, L. Reining, and A. Rubio, Rev. Mod. Phys. **74**, 601 (2002).
[35] M. Shishkin and G. Kresse, Phys. Rev. B **75**, 235102 (2007).
[36] G. Kresse and D. Joubert, Phys. Rev. B **59**, 1758 (1999).
[37] P. E. Blöchl, Phys. Rev. B **50**, 17953 (1994).
[38] J. P. Perdew, K. Burke, and M. Ernzerhof, Phys. Rev. Lett. **77**, 3865 (1996).
[39] J. Paier, M. Marsman, K. Hummer, G. Kresse, I. C. Gerber, and J. G. Ángyán, J. Chem. Phys. **124**, 154709 (2006).
[40] A. I. Liechtenstein, V. I. Anisimov, and J. Zaanen, Phys. Rev. B **52**, R5467 (1995).
[41] J. H. Petersen and M. Marsman, J. Phys.: Condens. Matter **18**, 7021 (2006).
[42] F. Fuchs, J. Furthmüller, F. Bechstedt, M. Shishkin, and G. Kresse, Phys. Rev. B **76**, 115109 (2007).
[43] S.-H. Wei, L. G. Ferreira, J. E. Bernard, and A. Zunger, Phys. Rev. B **42**, 9622 (1990).
[44] S. J. Cho, Phys. Rev. B **1**, 4589 (1970).
[45] A. Fleszar and W. Hanke, Phys. Rev. B **71**, 045207 (2005).
[46] T. Miyake, P. Zhang, M. L. Cohen, and S. G. Louie, Phys. Rev. B **74**, 245213 (2006).
[47] M. Shishkin, M. Marsman, and G. Kresse, Phys. Rev. Lett. **99**, 246403 (2007).